JAKU: Earth Sci., **Vol. 21,** No. 2, pp: 47-75 (2010 A.D. / 1431 A.H.)

DOI: 10.4197 / Ear. 21-2.3

Field, Mineralogical and Geochemical Characteristics of As-Sarat Laterite Profiles, SW Saudi Arabia

A.M.B. Moufti

Department of Mineral Resources and Rocks, Faculty of Earth Sciences, King Abdulaziz University, P. O. Box 80206, Jeddah 21589, Saudi Arabia

ambmoufti@hotmail.com

Received: 25/10/2008 Accepted: 23/12/2008

Abstract. Complete laterite profiles were developed over a variety of rocks including serpentinites, amphibolites and gabbroic bedrocks that are transected in most by ignispumite in the form of dykes and sills. The fresh bedrocks grade upwards into light gray saprolite, kaolinite, impregnated at its upper part by red iron oxides and capped by fluvial and slope-wash clastics laid over undulatory surface of recent erosion.

Ancient weathering profiles are well represented in East of Al-Wahaba, West of Al-Wahaba, Ash-Shara, Al-Qubal and Ad-Darama. These occurrences show lateral variation in elements composition during ancient weathering along a line extended from the North to the South of As-Sarat area. It points out to the excessiveness of K_2O over Na_2O values in the central part of the region and the excessiveness of Na_2O over K_2O values in the northern and in the southern parts. The behavior of trace elements suggest that during the early phase of weathering, small quantities of Na- and K-sulfates and chloride salts are formed in the upper horizons by virtue of capillary action. The weathering materials that originated from thermal alteration products are characterized by relative enrichment in oxides of Ti, Fe^{+3}, Fe^{+2}, Na and K, and depletion in Si, Al and Mg. Collectively, modern weathering in dry semi-tropical weather indicates that enrichment of iron content occurs at the expense of Si, Al and Mg. In addition, iron oxides (Fe^{+3} and Fe^{+2}) are enriched in the transition horizon between the saprolite and the top soil horizon, and associated with gain in CaO.

Trace elements (namely Cr, Cu and Ni) are allied to the ferric iron in the weathered scree-debris and allied to alumina and ferrous iron in the weathered basaltic blocks. The provided examples of modern weathering in dry semi-tropical weather deny the iron enrichment in laterite crust by capillary action and attribute it to subsurface laterite migration of ephemeral water, derived from rain and drainage streams, carrying soluble iron in the divalent state.

Introduction

As-Sarat region is located in the top of a highland cratonic region in the southwestern part of Saudi Arabia. It is situated between latitudes 17° 45' and 18° 20' N and longitudes 43° and 43° 30' E (Fig. 1), covering an area of about 859 km^2, running parallel to the general trend of the Red Sea axis. Laterites in the region have been developed over Precambrian tectonic belt (Greenwood *et al*., 1980). The so-called "As-Sarat laterite field" extends southward until the western scarp face of the Arabian Shield. The parent rocks are mainly composed of amphibolitic gneisses that were folded, and then intruded by large bodies of tonalite-granite gneiss during the Asir Orogeny (Schmidt *et al*., 1973). There is about 90 m thick sequence of clastic rocks resting on top of the Arabian Shield at As-Sarat region representing the Cambrian-Devonian Wajid Formation (Brown *et al*., 1989). This formation is exposed also over the Precambrian crystalline rocks at the eastern margin of the Arabian Shield.

Philby (1952) was the first to record and contribute to the occurrence of laterites in As-Sarat region, which were mapped by Brown and Jackson (1962). Some detailed works were carried out by Overstreet (1965 & 1966) who reported that the common minerals of laterites are smectite, chlorite, kaolinite, cristobalite, quartz, goethite and alunite. Much of the kaolinite is crystalline, quartz-free type was not found (Overstreet *et al*., 1973). Therefore, these laterites can not be considered as ores for iron or aluminum (Overstreet *et al*., 1977). Rooney and Al-Khoulak (1978) concluded that the laterite deposits of As-sarat Mountain area are unsuitable as raw materials for the manufacture of structural clay products. Odent and Al-Habashi (1981) reported that natroalunite is the major constituent confining to porcellanite veins in the laterites of As-Sarat mountains. They estimated a total reserve of laterite attaining 35 million cubic meters of mixed saprolite, laterite and porcellanite containing an average of 21% Al_2O_3. However, all of the above mentioned authors were interested in the suitability of the As-Sarat laterite for industrial applications without paying attention to ore genesis.

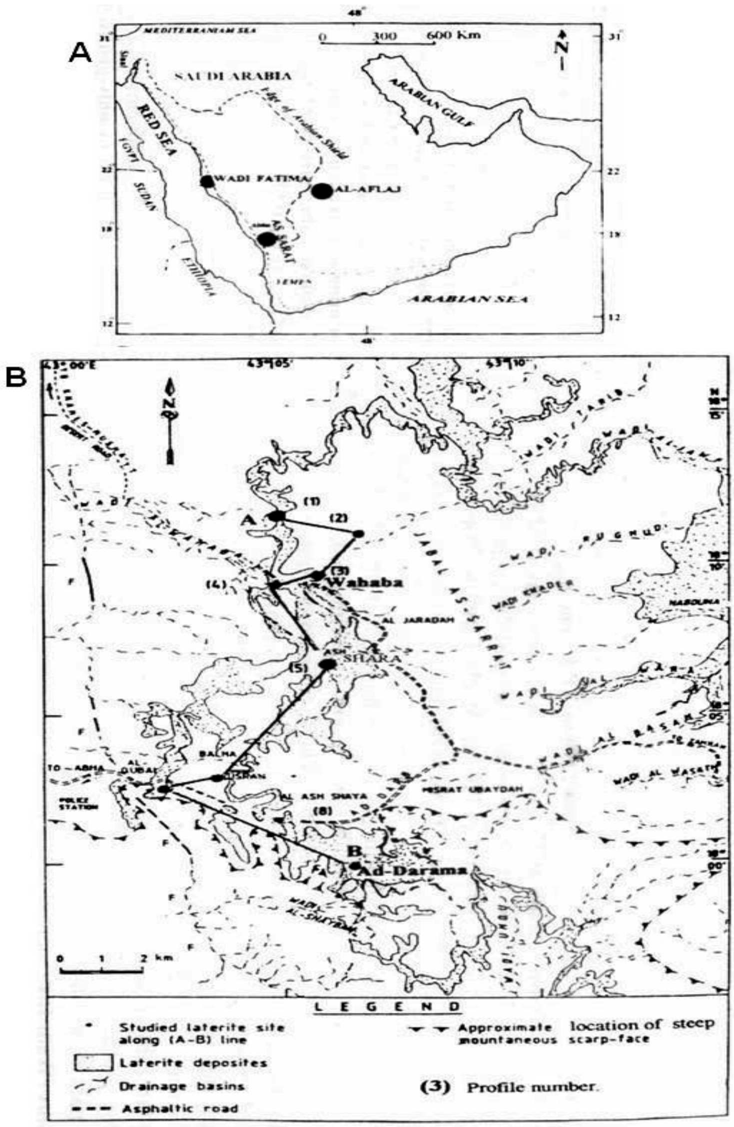

Fig. 1: (A) Location map of As-Sarat area. (B) Locations of the studied laterite profiles.

The main objective of the present study is to construct geochemical models that would help in differentiating the weathered materials that originate from fresh Quaternary basalt and those originating from thermally altered products.

Field and Laboratory Works

Geomorphological, sedimentological and geochemical studies were carried out to investigate eight (8) laterite profiles from As-Sarat area (Fig. 1). These profiles are assigned by successive numbers (1 to 8) running from the north to the south (Fig. 1 & 2). The profiles are named according to the geographic name of the valleys or the nearest village to each profile (Tables 1, 2 and Fig. 2). Locations, facies, nomenclature, age and dominant composition of the different laterite horizons are illustrated in Fig. 2. Care has been taken to collect complete lateritic sequence samples including all phases of weathering products and the original fresh rocks.

Table 1. List of the studied laterite profiles of As-Sarat mountain area.

No.	Local name	No.	Local name
1	North of Al-Wahaba	5	As-Shara
2	Al-Jowf	6	Al-Qubal
3	East of Al-Wahaba	7	Usran
4	West of Al-Wahaba	8	Ad-Drama

Table 2. Generalized description of the laterite profile developed in As-Sarat region.

Horizon	Horizon	Thickness (m)
Top soil	Oligocene-Miocene basaltic flow over porcellanite horizon of about 10-20 cm. in thickness. In some places (W. Al-Wahaba), this horizon is made of transported basaltic pebbles mixed with finer quartz and kaolin deposits with remarkable horizon of red hematite at the top.	0 – 15
Upper part of duricrust	Brown, hard spheroidal or nodular beans-type laterite imbedded in hematitic or siliceous and kaolinitic matrix.	1.3 – 2.1
Lower part of duricrust	Brownish yellow spheroidal or nodular ironstone (beans type laterite) embedded in soft yellowish goethitic matrix.	0.5 – 1.5
Mottled	Grayish white clay spotted with (1-5 cm) red iron oxide material, sometimes forming nodular ironstone which increase in frequency upward with ferrallitic and fersiallitic lenses in top. The pisoids made up of Na-chlorite, smectite, kaolinite and goethite. In Ash-Shara profile, the mottled horizon is overlain by saprolite horizon with clastic quartz grains, followed upward by pallid horizon, capped by spheroidal ironstone crust suggesting a Miocene-Recent intense weathering beneath the Mottled horizon (due to leaching in interfluves).	2 – 5
Pallid	White to purple kaolin with hydrous iron and aluminium oxides, occurs in profiles 3 and 5 of figure (3) and greenish gray illite and chlorite, in profiles 4, 6 and 8. This horizon laid in Al-Qubal locality (profile 6) over a 3.5 m. thick horizon of spheroidal (pisolitic) ironstone crowned by goethitic paleo-crust (1 m. thick).	8
Saprolite	Green color (serpentine minerals) rotten rock possesses the structure and the weathered dike materials of the underlying parent rock. Erosional surface character of smectite-chlorite spherules is common at the top of this horizon.	50
Parent rock	Precabrian fresh or thermally altered and deformed green-schist facies, intersected in some places by Triassic-Cretaceous felsic dikes.	

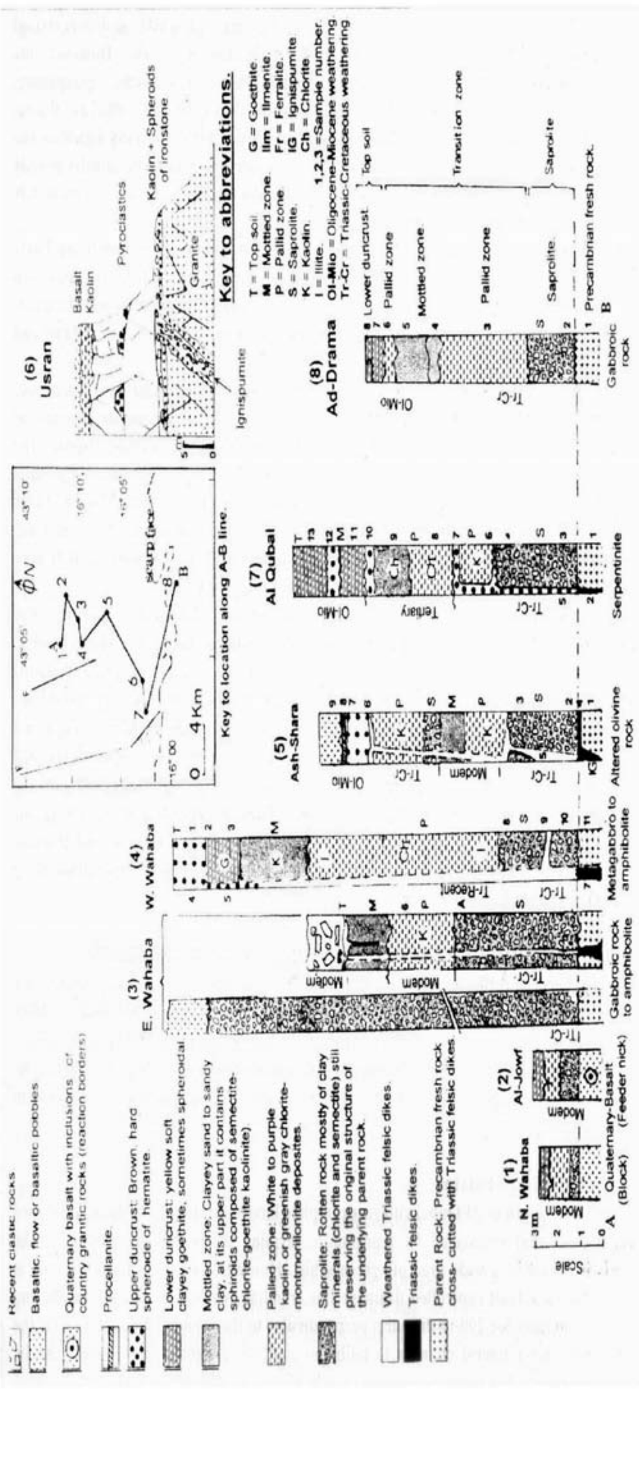

Fig. 2. Weathering profiles along (A – B) line in As – Sarat region, showing facies of the weathering horizons, mineralogy and reasonable age of lateralization.

A total of 47 samples representing both weathered samples and fresh crystalline fresh rocks were analyzed for major oxides and 8 trace elements, namely Cr, Cu, Ni, Pb, Ba, V, Cl and S. The analytical work was carried out at the laboratories of the Saudi Geological Survey (SGS) in Jeddah. For the measurement of major oxides, the X-ray fluorescence (XRF) technique was applied and the machine used is Model Bruker SRS 3400. The limit of detection of the major oxide is 0.1 wt % with the exception of MnO and SO_3^{--} that must attain the values of 0.01 and 0.05 wt %, respectively to enable the machine for their detection and consequently availability for their measurement. An ICP Optima 4300 DV machine was used for the measurements of trace elements, namely the incompatible elements, transitional and other heavy metals. A couple of rare-earth elements (REE), namely Ce & La were also measured by the same ICP machine that is housed at the Saudi Geological Survey.

The elemental composition of these samples are statistically correlated with the corresponding data of the shield-margin laterites (continental and littoral marine sediments). Identification of minerals in the studied laterite profiles was carried out using the X-ray diffraction technique. The results were obtained using a PW 1840 Philips diffractometer with Ni-filtered Cu Kα radiation at 30kV and 20 m A and normal scanning rate of 12θ/1cm/minute, housed at the research laboratories of Faculty of Earth Sciences, King Abdulaziz University. For the identification of both silicate and ore minerals in the investigated samples, selected Powder Diffraction Data for minerals documented in the ASTM electronic cards were used.

Geology of As-Sarat Area

The measured profiles of As-Sarat region represent the weathering products of basic and ultrabasic rocks from different geomorphologic and structural situations.

The parent rocks of the studied laterite profiles are made of dynamically and thermally altered crystalline rocks covered in few spots by Phanerozoic sedimentary sequences and all are crowned by Tertiary and Quaternary basalts. The prevailed crystalline rocks are mainly of para-gneisses and schists, undifferentiated granitic and granodioritic rocks and intermediate to mafic plutonic rocks. The rock of relatively lesser distribution on the top of the Shield is the Wajid Sandstone of Cambrian-Early Devonian to Permian age (Brown *et al*., 1989). It occurs at the eastern and the northwestern part of the study area. It is represented by 90 m thick sequence of massive sandstone with frequent quartz pebbles and granitic blocks at the base, in addition to spheroidal iron oxide materials at the top and over the base too.

In most cases, the laterite profiles are commenced at base by a thick saprolite horizon developed over irregular basal surface of weathering. The cap-rock of the laterite forms a summital free face of mesas rising 15-20 m above the incised valley bottom which is filled by reworked laterite. The valley bottom laterite covers most of the study area. Fortunately, complete weathering profiles of the valley bottom type are brought to light along fault planes of the Oligo-Miocene block faulting. It revealed subtle details of the parent rocks, the enclosed fresh dykes and the overlying saprolite, pallid horizon, mottled horizon and duricrust. A 50 m thick saprolite horizon was identified and measured in the southern part of the study area (Fig. 3).

The Tertiary basalts cover small mesas and many smaller flat-lying exposures (Fig. 3). Un-altered basaltic dykes are also present cutting through most of the lateritic profiles in As-Sarat occurrences. The basaltic rocks range in composition from hyperthene-normative basalt to alkalic picrite and alkalic olivine basalt. Age dating of two samples from As-Shara basalt sheet indicates 26 $\pm$ 3 Ma; talies of Oligocene age (Greenwood, 1985). The measured thickness of the Tertiary basalt is not exceeding more than 15 m. Nevertheless, a 50 m high Quaternary volcanic cone is recorded to the east of Al-Wahaba locality. Collectively, the crystalline rocks of the study area had suffered tectonic and thermal events that continued until the beginning of the Phanerozoic time. These events led to many cataclastic features. Teriary basaltic volcanism was probably localized by concurrent faulting and a fracture system. The Proterozoic fault planes were rejuvenated during the Tertiary times with brecciation along a major fault zone (Greenwood, 1985).

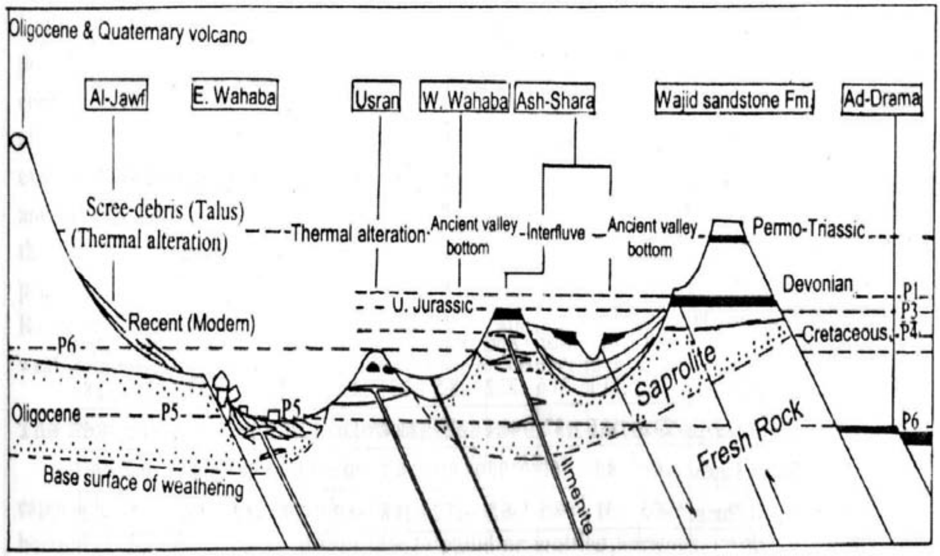

Fig. 3. Laterite formation and landform development in As-Sarat region. P1-P6 indicates profiles.

Field Description of the Studied Laterite Profiles

1. Al-Qubal Profile

Half kilometer to the south of Al-Qubal village, a complete laterite profile (12 m thick) was developed over a serpentinite bedrock that is transected by ignispumite in the form of dykes and sills (profile 7, Fig. 2). The serpentinite is included in a wide area of greenschists. However, the studied surface is generally sloped toward a fault-controlled drainage line trending NNW. The studied weathering profile extended laterally for 200 m, perpendicular to the drainage line. Moreover, the saprolitic horizon shows lateral changes to pallid or/and mottled horizons. This feature can be attributed to the effect of a relatively younger cycle of weathering on ancient saprolite that created the pallid and the mottled horizon due to lateral migration of drainage water (Fig. 4 and 5). Brown *et al.* (1989) reported that most NNW-trending faults in Sarat Ubida area are of Tertiary age (possibly along old rejuvenated fractures) where the weathering cycle possibly started during the Tertiary age.

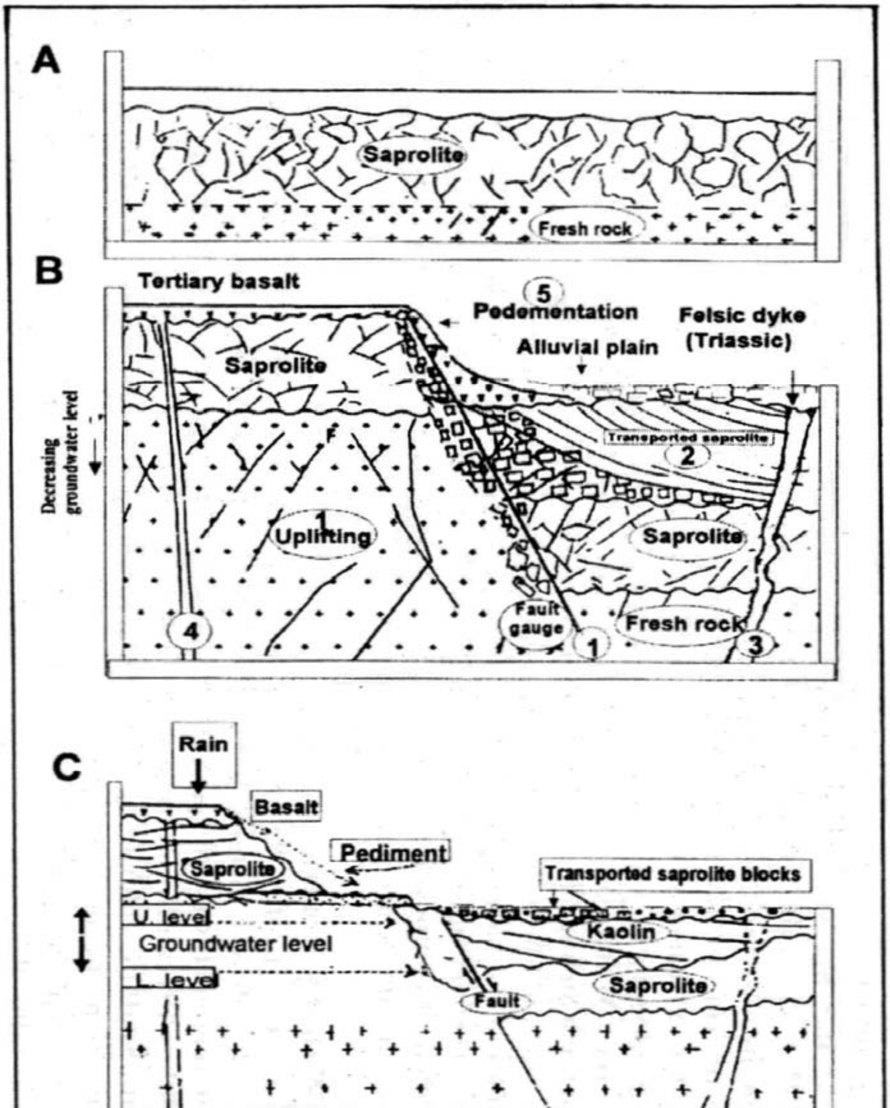

Fig. 4. Diagrammatic blocks showing sequences of events occurred during evolution of east Wahaba weathering profie.
(A) Early Triassic (or older) saprolitization,
(B) Sequential events are serialized in Arabic numbers into circles.
(C) Tertiary – Recent decrease in groundwater level, pediplanation, and kaolinization of transported saprolite.

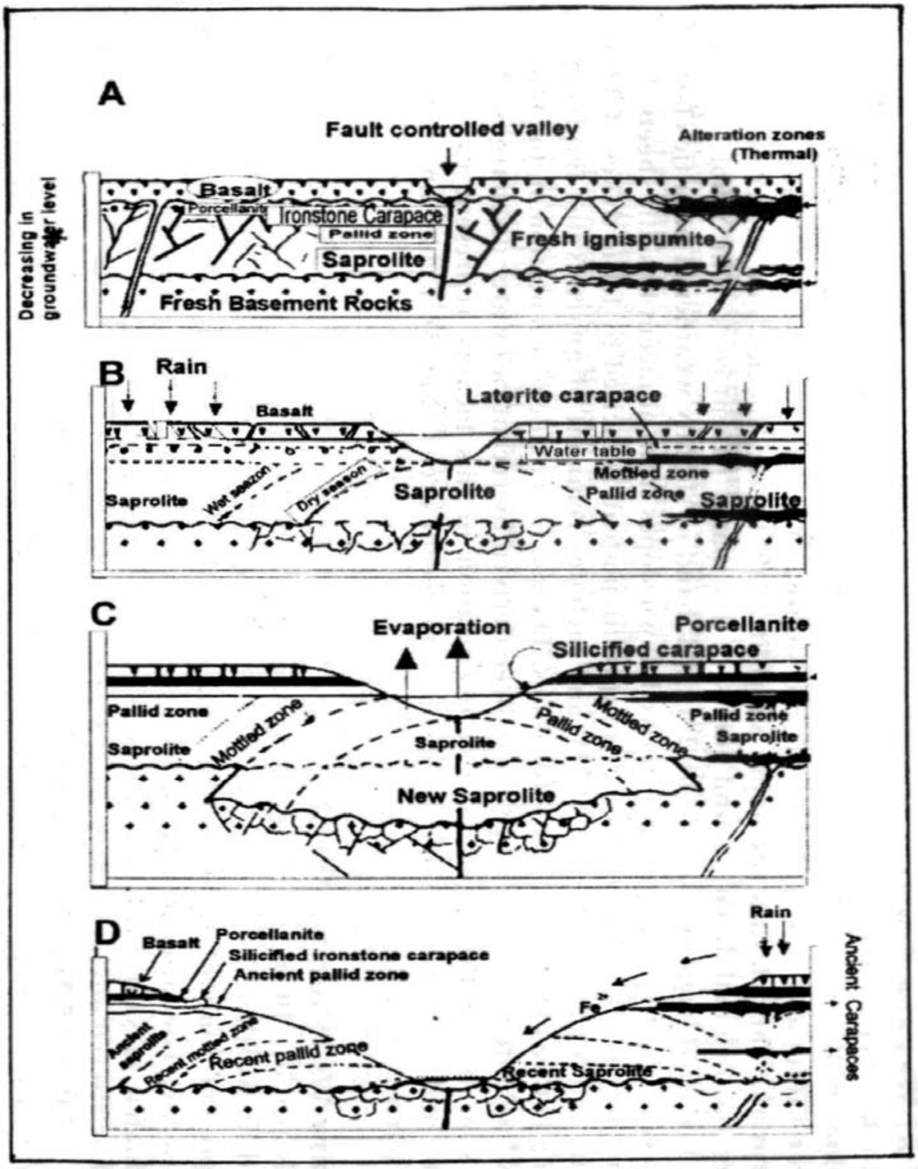

Fig. 5. Devopment of modern weathering profile from ancient saprolite.

(A) Uplifting extrusion of basalt flow, and initiation of a fault controlled valley.

(B) Effect of surface water, during wet period.

(C) Effect of surface water, during dry period.

(D) Present situation (Al Shara locality).

2. East of Al-Wahaba Profile

Two kilometers to the east of Al-Wahaba village, the fresh bedrock is gabbroic to amphibolitic grading upwards into light gray saprolite, kaolinite, impregnated at its upper part by red iron oxides and capped by fluvial and slope-wash clastics laid over undulatory surface of recent erosion (Profile 3, Fig. 2). These clastics include saprolite rubble and blocks, one meter in diameter, possessing the original foliation and joints of the basal parent-rock. The whole weathered sequence is unconformably overlain by a 2 m thick band of slightly weathered basaltic clasts (Fig. 2). The basaltic clastics are obviously derived down slopes from the nearby basaltic sheets that were laid over 50 m thick horizon of saprolite. This saprolite plateau is incised by felsic dykes of Triassic-Creataceous age (Overstreet *et al*., 1973), and includes trace of quartz veins implying deep weathering before extrusion of the felsic dykes. The red iron oxide pigmentation on the top of the light gray kaolinite horizon visibly has been derived by recent rainwater discharging from the up-slope saprolite to the valley floor. Lateritization in this locality represents two cycles of weathering and erosion, namely Triassic-Cretaceous and recent cycles (Fig. 2). Evolution of the entire profile is shown in Fig. 4.

3. Ash-Shara Profile

This 10 m thick profile represents an ancient mesa capped by a lateritic cover and transected by weathered basaltic dykes, and possibly surficial flows. It is located 1.5 km west of Ash-Shara village where higher level mesas represent remnant wall rock of ancient valley that are graded sideward into lower level valley bottom laterite (Profile 5, Fig. 2). The latter was developed as a result of intense weathering in the central part of the valley and graded to saprolite sideward (Fig. 5d). The parent rock is slightly altered and identified as altered olivine-rich rock (mostly dunite), intruded with felsic dykes (ignispumite), having an age of 248 $\pm$ 2.5 Ma, *i.e*. Permian-Early Triassic (Greenwood, 1985). The weathered dyke materials can also be traced upwards throughout the weathering profile. It is swept over its upper surface being peneplained and followed by an upper surface covered by red quartz clastics, followed upwards by ignimbrite (ash flow) that is weathered to reddish brown certified-beans lateritic crust capped by a thin horizon of porcellanite (about10 cm thick), and finally crowned by thin layer of Tertiary alkali basalt. However, two horizons of spheroidal iron oxides (pisolitic ironstone) are encountered in the lower and upper parts of the Ash-Shara profile. This weathering profile represents two cycles of weathering. The older one was supposed to have started after extrusion of the felsic volcanic dykes and ignimbrite, while the effect of the younger one is obvious in a relatively younger volcanic ash deposit covered by the Tertiary alkali basalt. The water surface flows of younger cycle of weathering, seems to be the paramount factor which led to the development of valley bottom laterite. The lower spheroidal ironstone horizon possibly represents the weathering products of earlier alteration border between the intruded ignispumite sill and the parent olivine-rich rock. The upper ironstone horizon lying underneath the Tertiary alkali basalt was formed in a reaction contact-border. Comparative diagrams illustrating chemical composition of iron rich horizons, either beneath the Tertiary basalt or juxtaposing the ignispumite are displayed and will be explained in a later section of the present paper.

4. West of Al-Wahaba Profile

This weathering profile is 18 m thick and is located 0.5 km to the west of Al-Wahaba village, being developed over metagabbro and amphibolite (profile 4, Fig. 2). It is bordered in the west by a regional fault scarp running northwest through the Khamis Mushayt area (Fig. 1 & 2). This fault scrap-face exhibits Precambrian metagabbro, which has been metamorphosed to the greenschist facies having foliated varieties that contain albite, chlorite, epidote and actinolite. The scrap-face now is eroded and the resulted slope of erosion is nearly clean with thin saprolite remnants filling joints over a steeply inclined peneplained surface. The weathering products were accumulated at the foothill as talus fault breccia, which developed later on into laterites. The lower horizon of the laterite profile is made up of 3 m thick horizon of saprolite including brown Ti-rich ferralite pockets. The pallid horizon consists of 8 m thick horizon of chlorite and illite followed upward by 3 m thick mottled horizon made up mainly of kaolinite. The upper horizon is composed of 1.9 m thick, dominated by goethite, irregularly capped with 1.2 m thick horizon of brown certified spheroids of ironstone with granularity ranging in size from 2 to 20 mm in diameter. Anderson (1979) reported that extensive faulting led to significant offsetting of the Cambro-Permian Wajid Sandstone in Khamis Mushayt area and it is older than the Tertiary basalt. Lateritization of the adjacent high-level laterites can then be assigned to a pre-Tertiary age; *i.e*. the time interval between Permian and Cretaceous. According to the peneplanation surfaces of the area and considering the upper most planation surface of the scrap face, weathering of west Al-Wahaba laterite probably has taken place during the Teriassic-Cretaceous time interval. The studied laterite profile is assigned to the valley floor-type as the effect of a relatively younger weathering cycle resulted in the formation of a complete laterite profile.

5. Ad-Drama Profile

A 9 m thick profile representing lateritic sequence was developed over gabbroic rocks, located 6 km to the south of Al-Qubal village at anonymous locality between Al-Massarah and Al-Aazep (Profile 8, Fig. 2). This weathering profile was developed over a detached fault-block that has been subsided for more than 300 m relative to the steep-scarp face of the Arabian Shield. The parent rock is altered and developed upwards into a 2 m thick weathered gabbro that still bear the original texture of the underlying rock. This is followed upward by 4 m pallid horizon composed of intensely disaggregated sand-sized grains of weathered gabbro graded into 4 m mottled horizon, made up of reddish brown clay with white spots, capped by 0.5 m of hard iron crust (porcellanite with metallic luster) and crowned at the uppermost top with a 0.3 m carapace of iron crust.

6. Usran Profile

The area east of Usran village is dominated by fresh ignispumite (ignimbrite) forming sills and dykes within pink fine-grained granite. The granite is capped by pyroclastics, which are crowned by a basaltic cover. Reaction rims (about 1 m thick) occur between the felsic volcanic rocks and the host granitic rocks. The weathering products of these contact-borders are intensely weathered giving rise to kaolinite as well as silicified pockets of spheroidal ironstone bodies with very characteristic pisolitic texture (2-30 mm in diameter). However, this site represents the base level of weathering and points out to possible derivation of spheroidal ironstone bodies from hydrothermally altered crystalline rocks.

Generalized Weathering Profile of the Laterites

During rock weathering on the top surface, the fresh parent rocks gradually decomposed from the surface downwards and four identifiable horizons were assembled, with more advancing weathering effect from top to bottom (Table 2). At the base of the weathering profile, saprolite up to 50 m. thick, is made up of permeable mixture of partially weathered rock bearing the original structure of the parent rock, together with clay, iron hydroxides and oxyhydroxides. The overlying pallid horizon, up to 8 m thick, is dominated by spherical masses of incompletely weathered rock floating into a clayey matrix. The overlying mottled horizon, up to 5 m thick, is dominanted by clays that also include rounded patchs of ironstone, 5-15 cm in radius. Sometimes, it contains iron pisoids with iron stained clays and quartz nets. The pisoids increase in frequency towards the top of this horizon. The upper horizon or the top soil horizon (up to 3.75 m thick), of fully developed weathering materials is a structureless mass of sandy clay mixed with yellow spherical masses of goethite (0.5-2 cm in radius). It is overlain by more condensed spherical bodies of brown goethite, usually sheltered by porcellanite that is truncated upwards by basalt. As mentioned in the section on laboratory work, minerals in the studied profiles were identified by X-ray diffractometry.

Geochemistry

The following part is devoted to the geochemical signatures of the laterite at As-Sarat region in order to shed some light on the behavior of different elements during lateritization. Examples for the modern and ancient weathering profiles from the on-shield laterite are all dealt with. Results of chemical analyses carried out for the different weathering profiles in the study area are provided in Tables from 3 to 7.

Table 3(a). Chemical composition of different horizons of Al-Qubal locality, As-Sarat Region.

	Horizon	Duricrust		Mottled	Pallid		Ancient Duricrust Saprolite				Parent Rock		
	13	12	11	10	9	8	7	6	5	4	3	2	1
SiO_2	32.11	30.20	33.19	33.30	37.03	37.58	59.73	38.14	64.42	34.65	43.10	49.33	48.54
TiO_2	1.85	3.26	2.79	1.6	0.26	0.28	0.91	1.91	0.11	0.24	0.17	1.54	0.01
Al_2O_3	26.10	18.10	15.38	17.07	32.77	28.7	18.16	23.49	20.60	17.91	21.55	13.69	20.05
Fe_2O_3	6.84	5.51	8.59	6.19	1.96	1.31	7.55	7.69	0.49	0.78	2.14	5.95	0.21
FeO	0.08	0.15	0.12	0.49	0.04	0.04	0.19	0.03	0.04	0.13	0.03	8.26	0.15
MnO	0.05	0.26	0.41	0.30	0.07	0.02	0.12	0.20	0.01	0.03	0.36	0.18	0.01
MgO	16.6	28.30	29.99	30.50	12.54	18.94	4.23	1.47	3.87	29.02	19.87	2.13	24.51
CaO	0.92	0.73	1.04	0.88	0.46	0.23	0.13	3.70	0.10	3.73	0.19	11.33	0.10
Na_2O	0.78	0.24	0.24	0.24	2.28	0.86	2.06	5.90	0.04	0.21	0.89	3.22	0.84
K_2O	0.61	0.21	0.29	0.28	1.37	0.18	0.14	1.49	0.12	0.15	0.19	0.71	0.05
P_2O_5	0.71	0.01	0.01	0.01	0.18	0.91	0.05	0.38	0.18	0.01	0.20	0.18	0.17
H_2O	1.58	1.37	0.60	0.58	0.72	0.41	0.15	0.65	0.11	0.53	0.71	0.15	0.84
LOI	11.30	11.10	6.97	8.53	9.03	10.43	6.14	14.36	8.21	12.40	10.16	2.08	4.20
Total	99.60	99.40	99.62	99.97	98.71	99.89	99.56	99.41	98.30	99.79	99.56	98.75	99.68
Cr	84.6	98.1	72	78.5	17.3	15.6	86.5	40.5	0.1	5.5	22.8	111.9	4
Cu	23.5	18.6	12.4	21.7	18.8	11	26.6	18.4	0.1	8.6	12.5	23.3	4.9
Ni	98	77	42	75	45.1	86	66	65	36	53	42	79	25
Pb	49	48	31	47	68.6	30	70	47	49	41	118	33	19
Ba	478	217	318	208	35.3	241	610	684	125	559	376	589	229
V	384	397	487	417	95	149	417	341	78	149	212	451	59
Cl	2200	3963	2205	1758	2474	1766	2638	3530	1319	2201	5302	5696	2638
S	596	462	370	339	936	355	402	417	328	546	537	388	515

Table 3(b). Samples identification.

No.	Description	No.	Description	No.	Description
Top		9	Chlorite	4	Saprolite gabbro
13	Yellow Tuff	8	Chlorite	3	
12	Pisolitic Kaolin in Chlorite	7	Spheroidal goethite	2	Amphibolite dyke
11	Pisolitic Kaolin in chlorite-dominated horizon	6	Goethite	1	Gabbro
10	Chlorite-dominated horizon	5	Altered Amphibolite		

Table 4(a). Chemical composition of laterite profile from Ash-Shara locality, As-Sarat region.

	Top Soil	Mottled Horizon		Parent Rock	Saprolite Horizon		
	7	6	5	4	3	2	1
SiO_2	16.47	17.01	39.37	43.18	30.28	53.77	48.79
TiO_2	0.59	2.69	1.14	0.32	3.12	0.02	0.02
Al_2O_3	16.06	16.37	22.54	18.95	18.30	15.52	19.13
Fe_2O_3	53.24	34.98	4.37	4.61	5.27	0.01	0.60
FeO	0.04	0.05	0.04	0.03	0.13	0.26	0.11
MnO	0.31	0.14	0.04	0.06	0.25	0.01	0.01
MgO	2.88	3.87	18.74	22.18	27.83	27.74	24.07
CaO	0.53	12.17	0.60	0.54	0.71	0.01	0.13
Na_2O	0.01	0.01	0.85	0.78	0.23	0.95	0.82
K_2O	0.07	0.01	0.41	0.34	0.20	0.05	0.34
P_2O_5	0.14	1.32	0.15	0.22	0.01	0.17	0.20
H_2O	0.07	0.14	0.27	0.40	0.16	0.04	0.33
LOI	8.65	9.95	11.16	7.02	12.27	0.36	4.78
Total	99.06	98.71	99.68	98.63	98.76	98.91	99.33
Cr	464	59	138	123	359	8	28
Cu	9	37	32	20	81	14	6
Ni	112	97	114	40	342	5	33
Pb	20	42	41	27	42	14	20
Ba	589	250	309	349	352	282	650
V	307	569	348	327	556	149	145
Cl	2653	3083	3093	3529	2194	2633	2630
S	500	537	434	951	415	470	428

Table 4(b). Samples identification.

No.	Description	No.	Description
Top			
7	Spheroidal ironstone (laterite)		
6	Intense weathered ignispumite		
3	Intensely weathered olivine rock	Bottom	
2	Saprolite	4	Fresh ignispumite
1	Altered olivine-dominated rock		

Table 5(a). Chemical composition of different horizons of West of Al-Wahaba weathering profile.

	Top soil			Pallid horizon			Saprolite			Parent rock	
	1	2	3	4	5	6	8	9	10	11	7
SiO_2	19.69	32.30	39.20	37.27	14.30	38.40	60.46	0.22	48.90	32.30	51.51
TiO_2	0.46	0.98	0.96	1.08	0.07	1.02	0.04	39.70	0.50	4.98	0.39
Al_2O_3	10.04	24.90	19.90	20.55	19.61	20.40	11.40	0.66	14.70	15.79	14.47
Fe_2O_3	59.67	7.74	7.26	7.49	23.78	6.58	15.67	10.10	6.35	16.07	4.93
FeO	0.03	0.03	0.01	0.01	0.01	0.02	0.21	4.91	4.82	1.12	3.70
MnO	0.09	0.06	0.05	0.06	0.05	0.04	0.03	4.23	0.17	0.53	0.16
MgO	1.21	17.00	18.80	19.32	2.00	19.40	9.47	1.95	2.98	10.23	2.74
CaO	2.05	0.81	0.81	0.86	1.89	0.81	1.73	26.70	13.30	5.44	13.67
Na_2O	0.04	0.73	0.85	0.87	0.01	0.90	0.01	0.05	3.74	0.80	3.53
K_2O	0.39	0.52	0.52	0.57	2.04	0.54	0.09	5.25	0.80	1.19	0.89
P_2O_5	0.38	0.13	0.12	0.15	1.43	0.15	0.33	0.08	0.13	0.32	0.15
H_2O	0.84	1.85	0.77	0.71	0.43	1.08	0.03	0.05	0.02	0.64	0.01
LOI	4.28	12.60	9.84	10.47	34.26	9.72	0.27	5.00	2.40	9.87	2.26
Total	99.17	99.50	99.00	99.41	99.88	99.00	99.74	98.90	98.80	99.27	98.41
Cr	14	279	394	147	96	170	8	495	246	205	65
Cu	5	50	13	24	65	21	21	15	14	25	24
Ni	26	264	86	75	47	63	17	305	138	113	98
Pb	35	46	28	25	51	31	2	28	40	32	36
Ba	221	240	203	164	194	180	135	565	430	259	588
V	232	406	331	335	101	282	35	362	349	270	349
Cl	1543	395	221	2207	10514	1323	2199	394	1765	3295	3532
S	416	625	430	405	1326	548	536	429	571	587	518

Table 5(b). Samples identification.

No.	Description	No.	Description
Top		8	Top dioritic horizon
1	Spheroidal laterite carapace	9	Titaniferous ferricrete
2	Laterite carapace	10	Altered diorite
3	Laterite carapace	11	Leached diorite
4	Extremely altered ignispumite	7	Slightly altered ignispumite
5	Deeply altered ignispumite	Bottom	
6	Altered ignispumite		

Table 6(a). Chemical composition of different horizons of Ad-Drama weathering profile.

	Duricrust			Transitional horizon			Saprolite	Parent rock
	8	7	6	5	4	3	2	1
SiO_2	26.66	10.71	37.56	19.43	40.32	29.75	44.04	43.82
TiO_2	1.46	1.05	1.75	0.24	0.95	0.16	0.34	0.14
Al_2O_3	13.76	5.33	21.70	20.09	12.41	15.23	14.91	16.67
Fe_2O_3	30.35	65.53	15.16	28.70	3.14	22.11	4.88	0.92
FeO	0.10	0.03	0.13	0.06	0.13	0.05	0.07	0.06
MnO	0.16	1.67	0.24	0.04	0.14	0.03	0.01	0.01
MgO	13.66	0.01	1.36	11.55	33.23	19.64	24.81	28.23
CaO	2.87	0.98	2.81	5.37	0.69	2.10	0.49	0.09
Na_2O	0.74	3.37	6.21	0.01	0.33	0.01	1.51	1.64
K_2O	1.47	1.32	2.00	0.47	0.21	0.57	0.71	0.15
P_2O_5	1.90	0.53	0.44	0.11	0.01	0.12	0.01	0.01
H_2O	0.33	0.19	0.09	0.09	0.31	0.28	0.27	0.19
LOI	6.53	8.50	9.64	13.53	7.94	8.44	7.16	7.02
Total	99.99	99.22	99.09	99.69	99.81	98.48	99.21	98.95
Cr	28	154	23	34	22	5	2	1
Cu	16	25	10	7	3	3	4	2
Ni	46	78	73	62	43	31	23	35
Pb	35	50	42	77	23	24	26	32
Ba	485	153	476	728	626	381	445	618
V	525	558	239	338	203	107	171	142
Cl	21576	2651	4417	2650	2640	1758	1764	2631
S	776	352	550	446	349	623	485	440

Table 6(b). Samples identification.

No.	Description	No.	Description
Top		4	Reddish brown chlorite-kaolinite
8	Siliceous ironstone crust	3	Intensely weathered gabbroic rock
7	Goethite	2	Weathered gabbroic rock
6	Na-Chlorite	1	Altered gabbroic rock
5	Brown smectite-chlorite*	Bottom	

- Identification of clays and other minerals was aided by XRD analysis.

Table 7. Chemical composition of different horizons of recently weathered basaltic materials and thermally altered mixture of basaltic and granitic materials (scree-debris) from As-Sarat region.

	Contact-border (thermal alteration)				Weathered basaltic block (WBB)			
	Upper	Transition	Lower	Average	Upper	Transition	Lower	Average
SiO_2	26.89	25.91	40.58	31.13	89.07	22.91	27.06	46.35
TiO_2	1.54	1.55	1.72	1.60	0.12	0.68	1.05	0.62
Al_2O_3	7.13	6.86	10.86	8.28	9.47	10.20	19.47	13.05
Fe_2O_3	41.05	42.14	17.62	33.60	0.01	40.93	31.47	24.14
FeO	4.01	4.14	0.08	2.74	0.43	3.80	0.05	1.43
MnO	0.18	0.22	0.02	0.14	0.01	0.18	0.35	0.18
MgO	0.01	0.01	2.14	0.72	0.01	1.74	2.70	1.48
CaO	4.32	4.60	3.37	4.10	0.10	13.37	0.42	4.63
Na_2O	6.89	6.06	0.03	4.33	0.01	0.10	4.46	1.52
K_2O	0.62	0.73	0.19	0.51	0.01	0.30	0.14	0.15
P_2O_5	0.22	0.19	0.16	0.19	0.01	1.34	0.11	0.49
H_2O	0.32	0.24	0.44	0.33	0.01	0.12	0.60	0.24
LOI	5.54	5.98	21.25	10.47	0.15	2.99	10.88	4.67
Total	98.72	98.63	98.46	98.79	99.41	98.66	98.76	98.94
Cr	298	264	192	394	12	11	872	298
Cu	70	75	47	64	26	23	53	34
Ni	261	3	146	137	24	42	99	55
Pb	32	31	26	30	12	35	66	38
Ba	599	613	417	543	195	661	37	298
V	433	413	329	392	125	187	668	327
Cl	2652	6175	2210	3679	2200	2190	1061	1817
S	414	373	321	369	342	490	1087	640

Vertical variation in the chemical composition within the weathering profiles is usually determined by comparison between values of the elemental composition in the fresh rock and the weathered residue (Caroll, 1970). This method imposes deletion of one of the essential elements from the operation. Several graphs are used that portray the individual variation of every element in the different horizons of each weathering profile. Figure 6 exemplifies the methods used in this paper. Assessment of loss or gain of elements in the different horizons, even alumina, can be achieved by visual correlation between representative thickness of every individual element in each horizon and the underlying horizon. Loss and gain of chemical elements during recent weathering of basalt (Fig. 6a), and during ancient weathering of thermal products of contact border materials (Fig. 6b & c) are illustrated and interpreted.

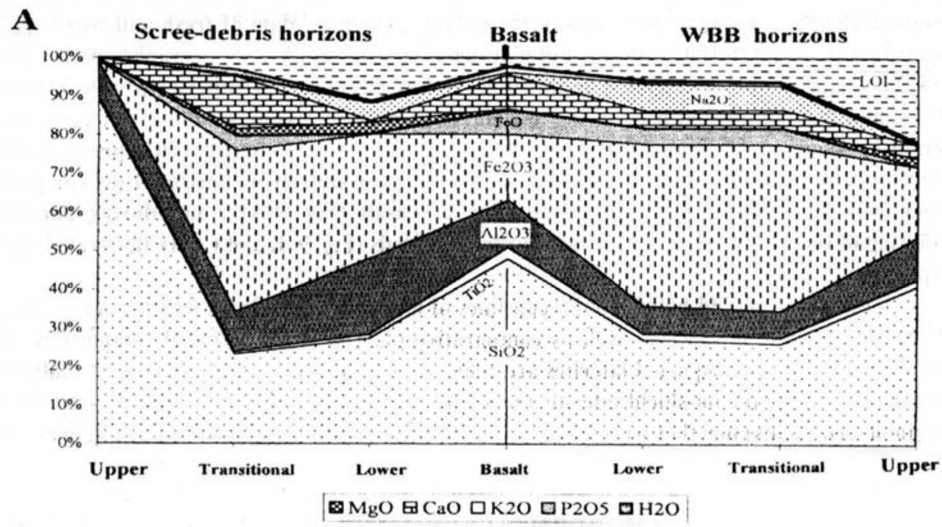

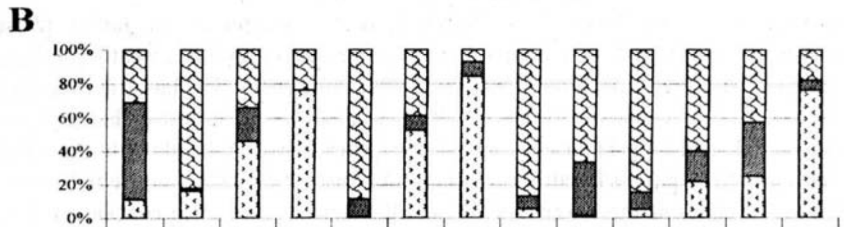

	SiO2	TiO2	Al2O3	Fe2O3	FeO	MnO	MgO	CaO	Na2O	K2O	P2O5	H2O	LOI
Top. Basalt	47.29	3'01	11.94	16.66	6.02	0.23	0.25	8.75	0.54	1.21	0.39	0.12	2.03
Porcellanite	89.26	0.06	6.94	0.01	0.73	0.05	0.29	0.76	0.26	0.15	0.12	0.09	0.68
Laterite	16.47	0.59	16.06	53.24	0.04	0.31	2.88	0.53	0.01	0.07	0.14	0.07	8.65

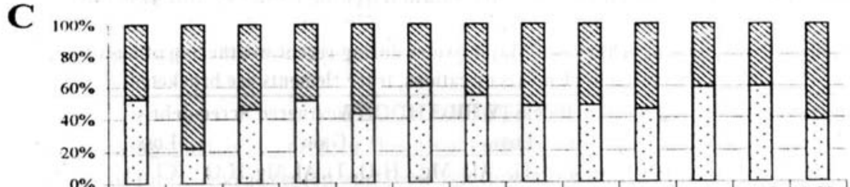

	SiO2	TiO2	Al2O3	Fe2O3	FeO	MnO	MgO	CaO	Na2O	K2O	P2O5	H2O	LOI
Weathered	39.37	1.14	22.54	4.37	0.04	0.04	18.74	0.60	0.85	0.41	0.15	0.27	11.16
Fresh Rock	43.18	0.32	18.95	4.61	0.03	0.06	22.18	0.54	0.78	0.34	0.22	0.40	7.02

Fig. 6: (A) Loss and gain in major oxides during recent weathering, relative to their percentage in the Quaternary fresh – basalt, Note WRR – Weathered basalt block B and C comparative diagrams between chemical composition of, (B) reaction rim (porcellanite) between basaltic sheet and ancient laterite, and (C) fresh and weathering products of ignispumite vein cross – cutting the Al – Shara weathering profile.

Lateral variation and polynomial trend-lines of major elements in all weathering profiles of As-Sarat region (Fig. 7), as well as comparative plots between chemical composition of residual laterites and transported laterites are achieved (Fig. 8). Principle component analyses (Tatsuoka, 1971) for the laterite with oolitic ironstone are computed and displayed in Fig. 8 & 9.

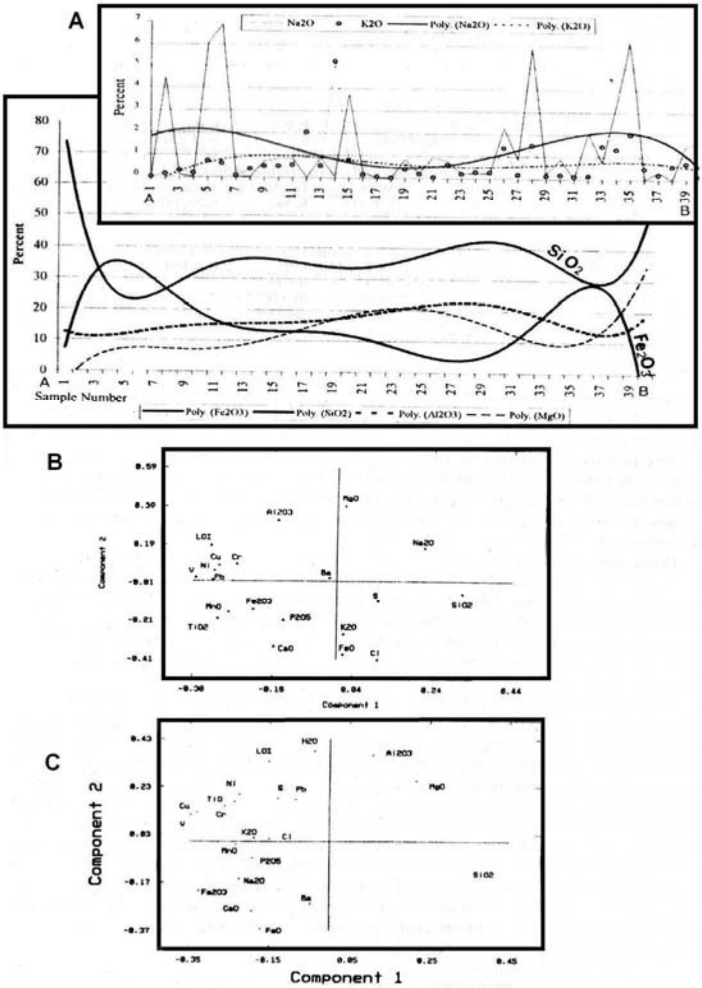

Fig. 7: (A) Variation and Polynomial trendiness of major elements composition of 39 weathering samples from As Sarat region, arranged from north to south (along A–B lines), B and C: Are two biplots of the first two principal components of recent (B) and (C) weathering samples from As Sarat region. (See text for explanation of element categories).

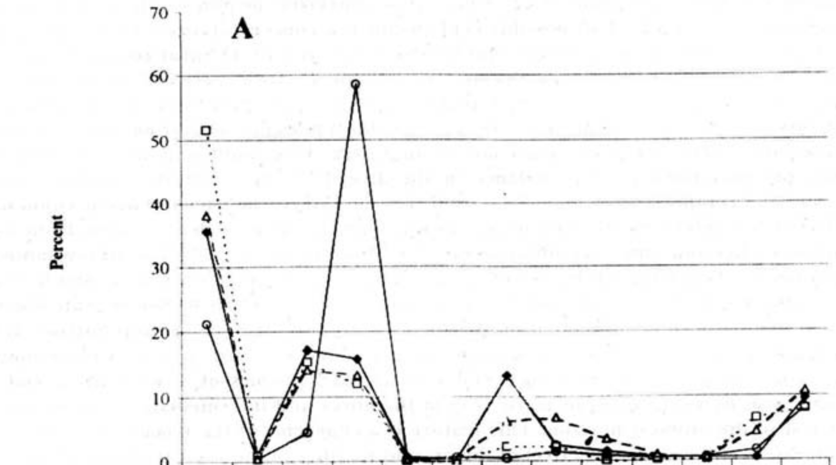

	SiO2	TiO 2	Al2O3	Fe2O3	FeO	MnO	MgO	CaO	Na2O	K2O	P2O5	H2O	LOI
As-Sarat	35.54	1.05	17.16	15.9	0.53	0.18	13.16	2.35	1.4	0.52	0.31	0.49	9.47
W. Fatima	51.55	0.82	15.36	11.9	0.07	0 03	2 17	2.16	0.03	0.28	0.21	6.56	7.94
Al Aflaj	38.18	0.44	14.3	13.41	0.17	0.09	6.1	6.75	3.48	0.98	0.46	4.51	10.76
Oolitic ironstone	21.33	0.48	4.4	58.66	0.13	0.59	0.44	1.51	0.75	0.44	0.68	1.63	8.14

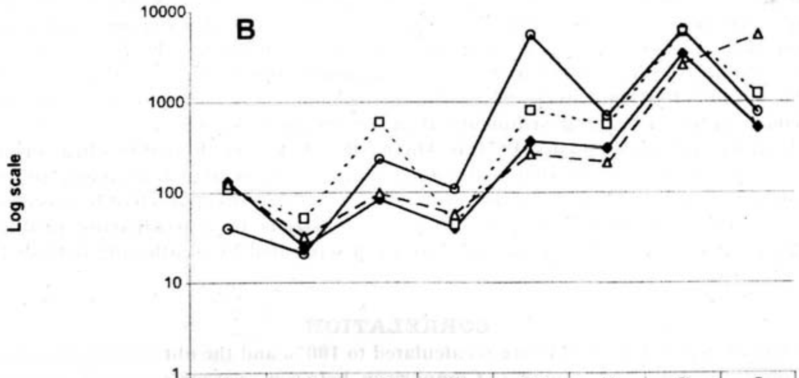

	Cr	Cu	Ni	Pb	Ba	V	Cl	S
As-Sarat	131.5	24.5	83.3	39.8	363.2	305.7	3370.9	515.6
W. Fatima	108.9	51.7	582.8	43.7	800.4	555.8	5943.8	1212.3
Al Aflaj	125.2	32	97.7	56.7	267.7	212.4	2555.4	5546.2
Oolitic ironston	39.4	20.8	231.5	108.8	5543	696	6322	761.8

Fig. 8. Mean chemical composition of residual on – shield laterites (As Sarat), shield margin transported laterite (wadi Fatima and Al Aflaj) and oolitic ironstone (Wadi Fatima).

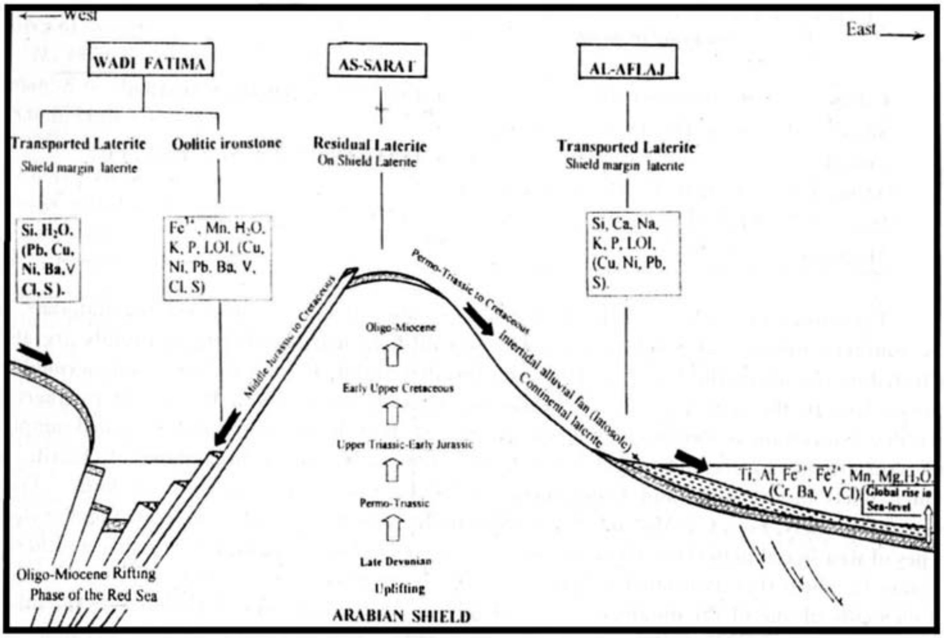

Fig. 9. Enriched elements in transported laterite and oolitic ironstone deposits relative to their mean values of residual laterite. Trace elements are bracketed.

Ancient weathering profiles are well represented in East of Al-Wahaba, West of Al-Wahaba, Ash-Shara, Al-Qubal and Ad-Darama locations. Figure 7(a) shows lateral variation in elements composition during ancient weathering along a line extended from the North to the South of As-Sarat area. It points out to the excessiveness of K_2O over Na_2O values in the central part of the region and the excessiveness of Na_2O over K_2O values in the northern and in the southern parts. The polynomial trendlines pointed to general inverse relationships between silica and iron contents, and general intimate relation between alumina and magnesia. This is due to the granitic composition in the central part and the basaltic composition in the north and in the south (De La Roche *et al*., 1980). On the other hand, recent weathering is represented at the basaltic blocks from North Al-Wahaba and Al-Jawf sites. The basaltic rocks in both sites are derived from the same source. Inspection of Fig. 6a indicates that iron (Fe_2O_3) is accumulated at the lower and the middle horizons, while silica is concentrated at the upper horizon of the recent weathered profiles. On the other hand, alumina is distributed evenly throughout the scree-debris with the intendance to accumulate either in the lower horizon of the weathered basaltic block or accompanying silica and magnesia in the upper horizon. Ferric iron oxide is enriched in the upper horizons of all laterites produced by ancient weathering. Enrichment in ferric iron oxide is positively correlated in the recent weathering profile and the ancient weathering too, where it is enriched in the lower and in the transitional horizons. Nervertheless, divalent iron enrichment in the lower and intermediate horizons of Ash-Shara and Al-Qubal profiles is attributed to weathering of the intruded dikes and sills. Enrichment of titanium is recorded in the top soil horizon of the recent and ancient weathering profiles, particularly in two profiles at Al-Jawf and Ad-Darama. It is evident that Ti-enrichment is controlled by the original mafic lithology that bears remarkable high percentages of Titaniferous pyrouxenes and Fe-Ti oxide ores, namely scree debris over basalt and gabbroic rocks at the two localities, respectively (Table 8). However, enrichment behavior of the rest of major oxides and trace elements during ancient and recent weathering are summarized in Table 8. This table shows diversity in ion types as being controlled by the original silicate mineralogy and the ore minerals present, particularly Fe-Ti oxides and minor sulphides.

Table 8. Enrichment of major oxides (as cation) and trace elements (in brackets) during ancient and recent weathering.

	Recent weathering		Ancient weathering			
Locality	N. Al-Wahaba	Al-Jawf	W. Al-Wahaba	Ash-Shara	Al-Qubal	Ad-Drama
Upper horizon	Si (Cr, Cu)	Si, Al, Ti, Mg (Ni, Pb)	Si, Al, Fe^{+3}, Ca, Na	Fe^{+3} (Ba)	Ti, Al, Fe^{+3}, Mn, P (Cr, Cu, V)	Ti, Fe^{+3}, Mn, P (Cr, Cu, Ni, V, S)
Transition horizon	Fe^{+3}, Fe^{+2}, Ca, K, P (Ba, Cl)	Fe^{+3}, Fe^{+2}, Ca, K (Cu, Ba, Cl)	Mg, K (Cr)	Al, Ca, K, P (Pb, Cl)	Fe^{+2}, Ca, K, Na (S)	Al, Ca, K, Na (Pb, Ba, Cl)
Lower horizon	Al, Fe^{+3}, Mg, Na (Cr, Cu, V, Pb, S)	Fe^{+3}, Na (Cr, Cu, Ni, V, Ba)	Ti, P (Cu, Pb, Cl, S)	Si, Ti, Fe^{+2}, Mg, Na (Cr, Cu, Pb, Ni, Cl)	Si (Cr, Pb, Ba, Cl)	Si, Fe^{+2}, Mg
Parent rock	Basalt	Scree-debris	Metagabbro to amphibolite	Altered olivine rock	Serpentinite	Gabbroic rock

The behavior of trace elements suggests that during the early phase of weathering, small quantities of Na- and K-sulfates and chloride salts are formed in the upper horizons by virtue of capillary action. In ensuring phase of weathering, the chloride salts are leached downwards to the middle horizon. Trace elements (namely Cr, Cu and Ni) are allied to the ferric iron in the weathered scree-debris and allied to alumina and ferrous iron in the weathered basaltic blocks. However, the weathering materials that originated from thermal alteration products are characterized by relative enrichment in oxides of Ti, Fe^{+3}, Fe^{+2}, Na and K, and depletion in Si, Al and Mg. Collectively, modern weathering in dry semi-tropical weather indicates that enrichment of iron content occurs at the expense of Si, Al and Mg. In addition, iron oxides (Fe^{+3} and Fe^{+2}) are enriched in the transition horizon between the saprolite and the top soil horizon, and associated with gain in CaO. Consequently, the provided examples of modern weathering in dry semi-tropical weather deny the iron enrichment in laterite crust by capillary action and attribute it to subsurface laterite migration of ephemeral water, derived from rain and drainage streams, carrying soluble iron in the divalent state. A simplified presentation of different elements enrichment is shown in Fig. 9. Generally, the relative enrichment in oxides of Ti, Fe^{+3}, Fe^{+2}, Na and K, and depletion in Si, Al and Mg originated from thermal alteration processes. It is evident that the excessiveness of K_2O over Na_2O values in the central part of As-Sarat region, and on the other hand the over dominancy of Na_2O over K_2O values in the northern and in the southern parts. Concerning the CaO accompanied by iron oxides (Fe^{+3} and Fe^{+2}), it seems that there are some enrichment in the transition horizon between the saprolite and the top soil horizon. In the weathered scree-debris over basalt, Cr, Cu and Ni follow the same behaviour of the ferric iron. On the other hand, these transitional metals (Cr, Cu & Ni) in the weathered basaltic blocks have the same behaviour of both alumina and ferrous iron.

Conclusions

1. Complete laterite profiles were developed over a variety of rocks including serpentinite, amphibolites and gabbroic bedrock that are transected in most by ignispumite in the form of dykes and sills.

2. The fresh bedrock grades upwards into light gray saprolite, kaolinite, impregnated at its upper part by red iron oxides and capped by fluvial and slop-wash clastics laid over undulatory surface of recent erosion.

3. Ancient weathering profiles are well represented in East of Al-Wahaba, West of Al-Wahaba, Ash-Shara, Al-Qubal and Ad-Drama occurrences show lateral variation in elements composition during ancient weathering along a line extended from the North to the South of As-Sarat area. It points out to the excessiveness of K_2O over Na_2O values in the central part of the region and the excessiveness of Na_2O over K_2O values in the northern and in the southern parts.

4. The behavior of trace elements suggest that during the early phase of weathering, small quantities of Na- and K-sulfates and chloride salts are formed in the upper horizons by virtue of capillary action. The weathering materials that originated from thermal alteration products are characterized by relative enrichment in oxides of Ti, Fe^{+3}, Fe^{+2}, Na and K, and depletion in Si, Al and Mg.

5. Collectively, modern weathering in dry semi-tropical weather indicates that enrichment of iron content occurs at the expense of Si, Al and Mg. In addition, iron oxides (Fe^{+3} and Fe^{+2}) are enriched in the transition horizon between the saprolite and the top soil horizon, and associated with gain in CaO.

6. Some transitional trace elements (namely Cr, Cu and Ni) are allied to the ferric iron in the weathered scree-debris and allied to alumina and ferrous iron in the weathered basaltic blocks.

7. The provided examples of modern weathering in dry semi-tropical weather deny the iron enrichment in laterite crust by capillary action and attribute it to subsurface laterite migration of ephemeral water, derived from rain and drainage streams, carrying soluble iron in the divalent state.

References

Anderson, R.E. (1979) Geology of Wadi Atf (sheet 17/34A) and Mayza (sheet 17/43) quadrangle, Kingdom of Saudi Arabia, *Directorate General of Mineral Resources Bulletin* **25**, 33 p.

Brown, G.F. and **Jackson, R.O.** (1962) Geological map of the Asir Quadrangle, Kingdom of Saudi Arabia, *United State Geological Survey*, *Misc. Geol. Inv. Map* 1-217 A, scale 1:500,000.

Brown, G.F., Schmidite and **Huffman, A.C. Jr.** (1959) Geology of the Arabian Peninsula. Shield area of western Saudi Arabia, *United State Geological Survey, Prof. Paper* No. **560**-A.

Caroll, D. (1970) *Rock Weathering*, Plenum Press, New York, p. 203.

De La Roche, H., Leterrier, J., Grandlaude, P. and **Marchal, M.** (1980) A classification of volcanic rocks using R_1 R_2 – diagram and major – elements analyses – Its relationship with current nomenclature., *Chem. Geol*., **20**: 183-210.

Greenwood, W.R., Anderson, R.E., Fleck, R.J. and **Robert, R.J.** (1980) Precambrian geologic history and plate tectonic evolution of the Arabian Shield, Saudi Arabian *Directorate General of Mineral Resources*, *Bulletin,* No. **24**: 35 p..

Greenwood, W.R. (1985) Geology map of the Bir Idmah quadrangle, sheet 18G, kingdom of Saudi Arabia, Directorate General of Mineral Resources, *Geoscience map GM-79C,* 1 pl., 1:250,000, with text, 30 p., 2 tab.

Odent, B. and **Al-Habashi, A.** (1981) *Alumina Tonors in Laterite and Saprolite from the As-Sarat Mountains, Saudi Arabia,* Ministry of Mineral Resources, Open Flile Report, BRGM – OF – 01 – 16, :39 p., 3 figures, 6 tables, 2 app.

Overstreet, W.C. (1965) Mineral investigation between Khamis Mushayt and Bir Idimah, Saudi Arabia, *United State Geological Survey Technical Letter* **23**: 15 p.

Overstreet, W.C. (1966) Preliminary results of a trip October 30-December 21, 1965, to the area between Shaya and Jabal Bani Bisqan, Saudi Arabia, together with a synopsis of mineral reconnaissance in the Asir quadrangle, *United State Geological Survey Technical Letter* **40**: 48 p.

Overstreet, W.C., Overstreet, E.F. and **Goudarzi, G.H.** (1973) *Mineralogical and Chemical Investigation of the Laterite in the As-Sarat Mountains, Kingdom of Saudi Arabia,* United State Geological SurveySaudi Arabian Project Report **46**: 66 p.

Overstreet, W.C., Overstreet, E.F. and **Goudarzi, G. H.** (1977) Tertiary laterite of As-Sarat Mountains, Asir Province, Saudi Arabia *Directorate General of Mineral Resources Bulletin* **21**: 24 pp, p.1, scale 1:1000,000, figs. 11.

Philby, H. and **St. J.B.** (1952) *Arabian Highlands*, Ithaca, New York, Cornell University Press for the Middle East Institute, 771 pp.

Rooney, L.F. and **Al-Khoulak, Z.** (1978) *Raw Materials for Structural Clay Products in the Abha-Khamis Mushayt Area, Kingdom of Saudi Arabia,* United State Gerological Survey Project Report 226, 39 pp.

Schmidt, D.L., Hadley, D.G., Greenwood, W.R., Gonzalez, L., Coleman, R.G. and **Brown, G. F.** (1973) Stratigraphy and tectonism of the southern part of the Precambrian Shield of Saudi Arabia, *Saudi Arabian Directorate General of Mineral Resources, Bulletin* No. **8,** 13 p.

Tatsuoka, M.M. (1971) *Techniques for Educational and Psychological Research.,* Wiley and Sons Inc., NewYork, p. 310.

المميزات الحقلية والمعدنية والجيوكيميائية لنطاقات لاتيريت السرات، جنوب غرب المملكة العربية السعودية

أسعد محمد بكر مفتي

قسم الثروة المعدنية والصخور، كلية علوم الأرض، جامعة الملك عبدالعزيز، ص. ب. ٨٠٢٠٦، جدة ٢١٥٨٩، المملكة العربية السعودية

المستخلص. تقع نطاقات اللاتيريت الكاملة بمنطقة السرات فوق مجموعة متنوعة من الصخور مثل السربينتينيت والأمفيبوليت والجابرو والمقطوعة في أغلب الأحيان بسدود وقواطع من الأجنيسبوميت. وتتدرج الصخور الأصلية إلى أعلى من سابروليت رمادي فاتح، ثم كاولينيت مرقط في أجزاءه العلوية بأكاسيد الحديد، ويلي ذلك غطاء من الرواسب النهرية والفتاتية المتكونة التي تقع علي سطح متعرج بفعل التعرية الحديثة.

وتوجد نطاقات التجوية القديمة بصورة واضحة في مناطق شرق وغرب الوهبة والشراع والقبال والظرمة، وهذه التواجدات توضح تغيرًا جانبيًا في تركيب العناصر أثناء التجوية القديمة من الشمال إلى جنوب منطقة السرات. وهذا يظهر في زيادة أكسيد البوتاسيوم على أكسيد الصوديوم في الجزء الأوسط من منطقة الدراسة، وعلى العكس تفوق نسب أكسيد الصوديوم على أكسيد البوتاسيوم في شمال وجنوب المنطقة. ويدل سلوك العناصر الشحيحة على أن كميات قليلة من كبريتات وكلوريدات الصوديوم والبوتاسيوم قد تكونت خلال الأطوار الأولى لعملية التجوية وذلك بفعل الخاصية الشعرية. وتتميز نواتج التجوية التي نشأت من التغير الحراري بإثراء نسبي في أكاسيد التيتانيوم والحديد الثنائي

والثلاثي والبوتاسيوم والصوديوم ويصاحب ذلك نزع لبعض عناصر السليكون والماغنسيوم والألمونيوم. و عموما، فإن التجوية الحديثة في طقس شبه مداري يدل على أن الإثراء في محتوي الحديد يحدث على حساب عناصر السليكون والماغنسيوم والألمونيوم. بالإضافة إلى ذلك، فان أكاسيد الحديد (الثنائية والثلاثية) حدث لها إثراء في النطاق الانتقالي بين السابروليت والتربة العلوية، ويرافق ذلك كسب في محتوي أكسيد الكالسيوم أيضًا.

وقد تبين أن بعض العناصر الشحيحة (الكروميوم والنحاس والنيكل) تتركز مع الحديد الثلاثي في فتات التجوية العلوي، ومع الألومينا والحديد الثلاثي في الصخور البازلتية التي تعرضت لعمليات التجوية. وتشير هذه الحالة من دراسة التجوية الحديثة في الطقس شبه المداري إلى إثراء الحديد في تربة اللاتيريت بفعل الخاصية الشعرية، ونتيجة الهجرة اللاتيريتية تحت السطحية بفعل مياه الامطار وروافد الصرف التي تحمل الحديد الذائب في صورته الثنائية.